RESEARCH ARTICLE

2-deoxy-D-Glucose Synergizes with Doxorubicin or L-Buthionine Sulfoximine to Reduce Adhesion and Migration of Breast Cancer Cells

Ebtihal H Mustafa[1], Huda T Mahmoud[2], Mariam Y Al-Hudhud[1], Maher Y Abdalla[3], Iman M Ahmad[4], Salem R Yasin[2], Ali Z Elkarmi[2], Lubna H Tahtamouni[2]*

Abstract

Background: Cancer metastasis depends on cell motility which is driven by cycles of actin polymerization and depolymerization. Reactive oxygen species (ROS) and metabolic oxidative stress have long been associated with cancer. ROS play a vital role in regulating actin dynamics that are sensitive to oxidative modification. The current work aimed at studying the effects of sub-lethal metabolic oxidative stress on actin cytoskeleton, focal adhesion and cell migration. Materials and Methods: T47D human breast cancer cells were treated with 2-deoxy-D-glucose (2DG), L-buthionine sulfoximine (BSO), or doxorubicin (DOX), individually or in combination, and changes in intracellular total glutathione and malondialdehyde (MDA) levels were measured. The expression of three major antioxidant enzymes was studied by immunoblotting, and cells were stained with fluorescent-phalloidin to evaluate changes in F-actin organization. In addition, cell adhesion and degradation ability were measured. Cell migration was studied using wound healing and transwell migration assays. Results: Our results show that treating T47D human breast cancer cells with drug combinations (2DG/BSO, 2DG/DOX, or BSO/DOX) decreased intracellular total glutathione and increased oxidized glutathione, lipid peroxidation, and cytotoxicity. In addition, the drug combinations caused a reduction in cell area and mitotic index, prophase arrest and a decreased ability to form invadopodia. The formation of F-actin aggregates was increased in treated T47D cells. Moreover, combination therapy reduced cell adhesion and the rate of cell migration. Conclusions: Our results suggest that exposure of T47D breast cancer cells to combination therapy reduces cell migration via effects on metabolic oxidative stress.

Keywords: F-actin - oxidative stress - metastasis - focal adhesion - glutathione

Asian Pac J Cancer Prev, **16 (8)**, 3213-3222

Introduction

Breast cancer is the most common cancer in women worldwide. It is the major cause of death from cancer among women globally (Mu et al., 2012). In 2014, an estimated 232,670 new cases of invasive breast cancer will be diagnosed in U.S. women. In addition to invasive breast cancer, an estimated 62,570 cases of carcinoma in situ (CIS) will be diagnosed (ACS, 2014).

Cancer metastasis represents the final, most advanced stage of malignancy and is the leading cause of death by cancer (Pani et al., 2010; Mu et al., 2012). Metastasis is a multistep process that includes a wide array of cellular changes involving alterations in cell structure by affecting cytoskeleton dynamics and expression of adhesion molecules (Mu et al., 2012; Lee and Kang, 2013; Meng and Yue, 2014).

Reactive oxygen species (ROS) are highly reactive molecules that are constantly produced in all aerobic organisms, mostly as a consequence of aerobic respiration (Ortega et al., 2010; Nourazarian et al., 2014). The term covers several types of chemical species, including free radicals such as superoxide (O^{2-}) or hydroxyl ($OH^{\cdot}$), and non-radicals such as hydrogen peroxide (H_2O_2) (Ortega et al., 2010). It has been reported that ROS contribute, in different ways, to carcinogenesis and to malignant progression of tumor cells (Pani et al., 2010; Nourazarian et al., 2014). The levels of ROS determine their effects on metastasis; where high levels suppress metastasis and destroy cancer cell directly or through the activation of apoptosis (Zhang et al., 2009), while the moderate levels induce cancer cell proliferation, migration, and invasion (Zhang et al., 2009). In addition, ROS play a vital role in

[1]Department of Physiology and Biochemistry, Faculty of Medicine, The University of Jordan, Amman, [2]Department of Biology and Biotechnology, Faculty of Science, The Hashemite University, Zarqa, Jordan, [3]Department of Pathology and Microbiology, College of Medicine, [4]Division of Radiation Science Technology Education, University of Nebraska Medical Center, Omaha, Nebraska, USA
**For correspondence: lubnatahtamuni@hu.edu.jo*

regulating actin dynamics, which is sensitive to oxidative modification (Barth et al., 2009).

Previous studies suggest that cancer cells produce more ROS than normal cells (Schumacker, 2006). 8-hydroxy-2-deoxyguanosine (8-OH-DG), which is the major oxidized modified DNA damage, has been reported to be at higher contents in human renal cell carcinoma than in non-tumorous tissue (Toyokuni et al., 1995; Nourazarian et al., 2014). Also, high levels of H_2O_2 and O^{2-} have been reported in several human carcinoma cell lines, including malignant melanoma, colon carcinoma, pancreatic carcinoma, neuroblastoma, breast carcinoma, and ovarian carcinoma (Toyokuni et al., 1995).

The level of ROS is determined by a balance between ROS generation and detoxifying system (Nakashima et al., 1984), where the imbalance between the oxidants and antioxidants could lead to oxidative stress (Sies, 1997). In order for cells to protect themselves against the damaging effects of ROS, they have evolved enzymatic antioxidants such as super oxide dismutase (SOD), catalase (CAT), heme oxygenase-1 (HO-1) and glutathione peroxidase (GPx) (Steinbrenner and Sies, 2009), and non enzymatic antioxidation mechanisms such as glutathione (GSH) (Wu and Cederbaum, 2003). However, many studies revealed that tumor cells have lower Mn-SOD, CuZn-SOD, and CAT activities when compared to their normal cells counterparts (Oberley and Buettner, 1979; Gurudath et al., 2012). In addition, it has been proposed that GPx activity is highly variable in different tumor tissues (Toyokuni et al., 1995; Gurudath et al., 2012).

Accordingly, cancer cells should have mechanisms other than the enzymatic antioxidant to resist oxidative stress. It has been reported that the metabolism of glucose and cellular pools of glutathione are involved in the protection of cancer cells against exogenous exposure to the hydroperoxide toxicity (Averill-Bates and Przybytkowski, 1994; Hegde et al., 2013).

Glutathione is the major endogenous antioxidant (Muyderman et al., 2004). GSH is synthesized via two enzymes: glutamate cystein ligase (GSL), which is the rate limiting reaction and inhibited by L-buthionine sulfoximine (BSO), and glutathione synthetase (GS) (Meredith and Reed, 1982; Green et al., 2006).

Glucose metabolism is thought to be involved in cellular sensitivity to oxidative stress mediated by hydroperoxide, presumably via the formation of pyruvate and NADPH (Lee et al., 1998). In this scenario, pyruvate reacts directly with H_2O_2 resulting in decarboxylation of pyruvate to acetic acid and reduction of H_2O_2 to H2O (Ahmad et al., 2005; 2010). NADPH is the source of the reducing equivalents for the glutathione/glutathione peroxidase/glutathione reductase system (Coleman et al., 2008).

Recently, it was discovered that the pharmacologic inhibition of glycolysis with 2-deoxy-D-glucose (2DG; a structural analogue of glucose) induced cytotoxicity in MCF-7 breast carcinoma cell line via metabolic oxidative stress (Lin et al., 2003; Lee and Kang, 2013). We have also shown that the combination of 2DG and doxorubicin (DOX) resulted in a significant cell killing in rapidly dividing T47D cells compared to 2DG or DOX alone (Ahmad et al., 2010). In addition, BSO sensitized these cells to the cytotoxicity of the combination of 2DG and DOX (Ahmad et al., 2010).

DOX is an effective therapy that has been used to treat cancers for more than 30 years (Takanashi and Bachur, 1976). However, the chronic side effects of DOX, the most detrimental is cardiomyopathy, limit the amount of this drug that can be given to patients (Takanashi and Bachur, 1976; Bertazzoli et al., 1979; Siveski-Iliskovic et al., 1995; Gille and Nohl, 1997; Zhou et al., 2001; Wold et al., 2005). DOX-causing cardiomyopathy is believed to be redox generated (Wold et al., 2005). Therefore, decreasing the amount of DOX given to patients using combination therapy such as 2DG or BSO which inhibit critical aspects of thiol-mediated hydroperoxide metabolism, leading to increased steady-state levels of ROS, might suppress vital steps during metastasis which could lead to highly desirable outcomes of therapy.

The current work aimed at studying the effects of sub-lethal metabolic oxidative stress mediated by combination therapy (2DG/BSO, 2DG/DOX, or BSO/DOX) on actin cytoskeleton, focal adhesion and cell migration in T47D human breast cancer cells.

Materials and Methods

Cell culture condition

T47D human breast cancer cells were cultured in a 1:1 mixture of High Glucose Dulbecco's Modified Eagle's medium and Ham's F12 medium (HGDMEM:F12; Lonza, Belgium) supplemented with 10% fetal bovine serum (FBS) (Euroclone, Italy), 1% L-glutamine (Lonza, Belgium), 1% penicillin/streptomycin (PAA, Austria), and 15 mM HEPES (Sigma Aldrich, USA) at 37°C in a humidified 5% CO_2 incubator (NUAIRE, USA).

Drug treatment

2DG, BSO and DOX were obtained from Sigma Aldrich. Drugs were added to cells at a final concentration of 20 mM, 1.0 mM and 0.1 μM, respectively. Stock solutions of 2DG and BSO were dissolved in phosphate buffered saline (PBS, pH 7.5), while DOX was dissolved in normal saline (0.9% NaCl). The required volume of each drug was added directly to complete cell culture medium to achieve the desired final concentration. All experiments were performed 24h post treatment.

Glutathione assay

Total glutathione (GSH+GSSG) content in control and treated T47D cells was measured according to Anderson (Anderson, 1985). The method depends on the colorimetric reaction of 5, 5-dithio-bis-2-nitrobenzoic acid (DTNB) with GSH to form 5-thio-2nitrobenzoic acid (TNB). The rate of TNB formation is proportional to the sum of GSH and GSSG present. GSSG is reduced to GSH by glutathione reductase (GR) and NADPH.The rate of TNB formation was determined at 412 nm, every 10 sec for 2.5 min using Jasco-V-530 spectrophotometer.The amount of GSSG in the sample was determined according to (Griffith, 1980). The reduced GSH was determined by subtracting the GSSG content from the total GSH. All

biochemical determinations were normalized to the protein content using the Bradford method.

Lipid peroxidation assay

Lipid peroxidation was determined by measuring thiobarbituric acid-reactive species (TBARS) as described by Ohkawa et al. (1979) with modifications. Cells were washed with ice-cold PBS, scraped into cold PBS and centrifuged for 5 min at 15,000 rpm. Cell pellet was homogenized in 250 µL 1% sodium dodecyl sulfate (SDS; BDH, England), and 1 ml of 20% trichloroacetic acid (TCA; Sigma Aldrich, USA). 2 ml of 0.8% thiobarbituric acid (TBA; ACROS, USA) and 250 µL of 1% phosphoric acid were added to the homogenate. The mixture was then boiled for 1 h, cooled on ice and then extracted with 1 ml n-butanol. The mixture was centrifuged briefly, and the absorbance of the upper phase was then measured at 530 nm with Jasco-V-530 spectrophotometer (Gavino et al., 1981; Lykkesfeldt, 2007). The values are expressed in nmole/mg protein malondialdehyde [MDA; end product of lipid peroxidation (Nourazarian et al., 2014).

Cell proliferation assay (MTT assay)

Proliferation assay is widely used as an indicator of cell metabolic viability (Coleman et al., 2008). Cell proliferation assay (MTT assay) was performed according to the method of Mosmann (Mosmann, 1983) with modifications. Briefly, 5×10^4 viable cells were seeded in the wells of a 96-well tissue culture plate containing growth media supplemented with FBS. Cells were kept in a humified 5% CO_2 incubator at 37°C for 24h. Freshly prepared MTT salt (5 mg/ml in PBS) (3-(4,5-dimethylthiazol-2-yl)-2,5-diphenyl tetrazolium bromide) was added to each well to give a final concentration of 0.5 µg/µl. The plates were incubated for 4 h and the formation of formazan crystals was checked using an inverted microscope. Equal volume of 1:1 (200 µl) mixture of dimethyl sulfoxide (DMSO; TEDIA Co., USA) and isopropanol was added to each well and incubated for 30-45 min. Cell viability was evaluated by measuring the absorbance at 570 nm using a Jasco-V-530 spectrophotometer. The percentage of survival was calculated as the proportion between absorbance of treated and control cells.

Cell fixation and immunostaining

T47D cells were plated on sterile glass cover slips at density of 1×10^4. Twenty four h post drug treatment, cells were fixed with 4% paraformaldehyde (Sigma Aldrich, USA) in cytoskeleton buffer with sucrose (CBS) [10 mM MES, pH 6.1, 138 mM KCl, 3 mM $MgCl_2$, 10 mM EGTA, 0.32 mM sucrose] for 45 min at room temperature. Cells were then washed three times five min each with 0.1% Triton X-100 in PBS.

To visualze actin cytoskeleton, F-actin was stained with fluorescent-conjugated phalloidin (Invitrogen, USA) in CBS for 1h. To visualize adhesion structures, cells were incubated with anti-paxillin antibody (BD Pharmingen, USA) [1:250 in 2% bovine serum albumin (BSA) in CBS] for 1 h and then with fluorescent-conjugated goat anti-mouse IgG (1:400 in 2% BSA in CBS) for 1h. Finally, cells were washed three times five min each with 0.1% Triton X-100 in PBS and mounted with Prolong Gold Antifade with DAPI (Invitrogen, USA). Images were captured using either a 40× NA 0.65 or 100× NA 1.3 objectives on an inverted Nikon microscope with a CCD camera.

Western blot analysis

Cells were lysed in cold lysis buffer (2% SDS, 10 mM Tris pH 7.5, 10 mM NaF, 2 mM EGTA, 10 mM dithiothreitol). Cell extracts were heated in a boiling water bath for 5 min and sonicated. Aliquots of lysates were diluted in 4x SDS-PAGE sample buffer (0.5 M Tris-HCl pH 6.8, 2% SDS, 20% glycerol, 20% 2-mercaptoethanol and 0.16% bromo-phenol blue) and proteins were resolved by electrophoresis on 10% SDS-polyacrylamide gels. Proteins were transferred onto nitrocellulose membranes and were blocked using 1% (w/v) BSA in Tris-buffered saline (TBS), and exposed overnight at 4°C to the primary antibodies [mouse GAPDH (1:6000; CHEMICON, USA), rabbit heme oxygenase-1 (HO-1; 1:2000; Sigma Aldrich, USA), rabbit MnSOD (1:1000; Sigma Aldrich, USA) and mouse catalase (1:2000; Sigma Aldrich, USA)] diluted in 1% BSA in TBS containing 0.05% Tween 20. After washing and incubation with appropriate secondary antibodies conjugated to horseradish peroxidase, the membranes were washed and the bands were visualized using the 3,30,5,50 tetramethylbenzidine system (TMB; Sigma, USA). Signals were quantified using TotalLab software (Nonlinear Dynamics).

Cell adhesion assay

Cells were plated on ice-cold freshly prepared collagen I (10µg/ml) (Sigma Aldrich, USA) -precoated 12 well tissue culture plate at a final concentration of 5×10^4/well (Estornes et al., 2007). Each well was treated with 150 µl collagen I, left for 1 h at 37oC incubator and then washed three times with PBS. Cells were incubated at 37°C on collagen I for 1 h and washed twice with PBS. Adherent cells were fixed with 4% paraformaldehyde for 30 min at room temperature, stained with 1% methylene blue (Gurr Certistain, England), diluted in 1 % Borax for 30 min at room temperature. After solubilization with 1% SDS, absorbance at 630 nm was measured.

Invadopodia assay

Ethanol-flamed sterile 18 mm glass coverslips were placed on the wells of 12-well tissue-culture plate and were coated with 50 µg/ml poly-L-lysine for 20 min at room temperature. The coverslips were covered with 0.5% glutaraldehyde for 15 min, and then were coated with 37oC-preheated 0.2% gelatin (Sigma Aldrich, USA) and Alexa Fluor 488 or 568-gelatin (Invitrogen, USA) mixture at a 8:1 ratio for 10 min at room temperature. The residual reactive groups in the gelatin matrix were quenched with 5 mg/ml sodium borohydride for 15 min at room temperature. Cells were plated at a concentration of 2×104/coverslip and incubated at 37°C for 6h. Finally, cells were stained for F-actin with fluorescent phalloidin (Artym et al., 2009).

Wound healing assay

T47D cells were grown on 6-well tissue culture plate to about 80% confluency. Cultures were wounded by a heat polished glass pipette (~ 30-50-µm tip) and overlayered with dimethyl polysiloxane (Sigma Aldrich, USA) to reduce evaporation while allowing gas exchange. Detailed observation on the behavior of live cells was monitored and the effects of the different drug treatments were assessed by measuring the time and the distance migrated by cells to close the wound. Live cell migration in wound-healing assay was followed using a CCD camera operated by Nikon ECLIPSE Ti widefield microscope equipped with a 37°C stage and 5% CO_2.

Migration assay

Control and treated T47D cells (1×10^6) were seeded into the upper compartment of a 12-well chemotaxis chamber (Neuroprobe, Gaithersburg, MD). Both the upper and lower compartments were filled with HGDMEM:F12 containing 0.35% BSA and were physically separated by a polycarbonate membrane (8-μm pore size) precoated for 4 h with 100 μg/ml collagen I. Cells were then incubated for 6h at 37°C in 5% CO_2 humidified conditions. Cells were fixed with 4% paraformaldehyde, and stained with 1% borax and 1% methylene blue. Cells of the upper surface of the filter were removed with a cotton swab, and those underneath were quantified (Estornes et al., 2007; Mu et al., 2012).

Statistical analysis

Statistical analysis was performed using STATISITCA 7 analysis program (StatSoft Inc., Ok, USA). To determine differences between 3 or more means, one-way ANOVA with Fisher's LSD for multiple comparisons post-tests were performed. Results are presented as mean±standard error of the mean (SEM). All statistical analysis was performed at $p<0.05$ level of significance.

Results

Combination therapy causes disruption in intracellular thiol pool

The changes in intracellular total glutathione (TGSH; GSH+GSSH) levels were measured in T47D human breast cancer cells treated with 2DG, DOX, and BSO individually or in combination for 24h. Figure 1A shows that individual drug treatment caused a significant decrease in total glutathione compared to untreated control cells, and that two drug combinations (2DG/BSO and BSO/DOX) enhanced TGSH depletion compared to individual drug treatment (Figure 1A). In addition, drug combinations caused a significant increase in % GSSG (oxidized glutathione) compared to control cells and to individual drug treatment (except for 2DG/DOX) (Figure 1B). We have shown previously that the effects of these drugs on intracellular glutathion pool was mediated by disruption in thiol metabolism and thus oxidative stress (Ahmad et al., 2010). Lipid peroxidation is the hallmark of oxidative stress (Wu and Cederbaum, 2003), thus malondialdehyde (MDA) level (secondary product of lipid peroxidation) was measured. As shown in Figure 1C, MDA levels were significantly elevated in treated cells. In addition, all of the drug combinations (2DG/BSO, 2DG/DOX or BSO/DOX) caused a significant increase in MDA levels when compared to individual drug treatment (Figure 1C).

Drug combination causes sub-lethal T47D cytotoxicity

T47D cells were treated with the different drugs individually or in combination and cell viability was measured using the MTT-based cell viability assay (Figure 2A). Our data show that individual drug treatment had a sub-lethal cytotoxity effect (around 20% reduction in cell viability) on T47D cells, which was more profound with drug combination (around 30% reduction in cell viability) (Figure 2A). BSO/DOX drug combination was the only combination that caused a significant increase in cytotoxity when compared to individual drug treatment (BSO or DOX alone) (Figure 2A).

Heme oxygenase-1 is induced in treated T47D breast cancer cells

To study the effects of TGSH depletion on the oxidative status of treated T47D breast cancer cells, the expression of three major antioxidant enzymes (CAT, HO-1, and MnSOD) was studied by immunoblotting (Figure 2B, C). Drug treatment (individually or in combinations) induced the expression of HO-1 as compared to control,

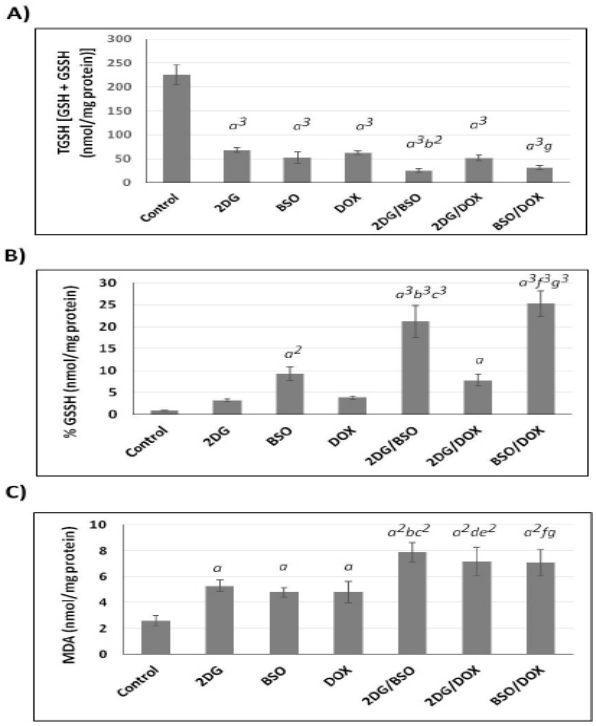

Figure 1. Thiol Metabolism is Disrupted in T47D-Treated Cells. T47D breast cancer cells were treated for 24h with individual or combination drugs and TGSH **(A)**, percentage of oxidized glutathione (%GSSG) **(B)**, and lipid peroxidation (MDA) **(C)** were measured. Three independent experiments. a $p<0.05$; a^2 $p<0.01$; a^3 $p<0.001$ versus control, b $p<0.05$; b^2 $p<0.01$; b^3 $p<0.001$ 2DG/BSO versus 2DG alone, c^2 $p<0.01$; c^3 $p<0.001$ 2DG/BSO versus BSO alone, d $p<0.05$ 2DG/DOX versus 2DG alone, e^2 $p<0.01$ 2DG/DOX versus DOX alone, f $p<0.05$; f^3 $p<0.001$ BSO/DOX versus BSO alone, g $p<0.05$; g3 $p<0.001$ BSO/DOX versus DOX alone

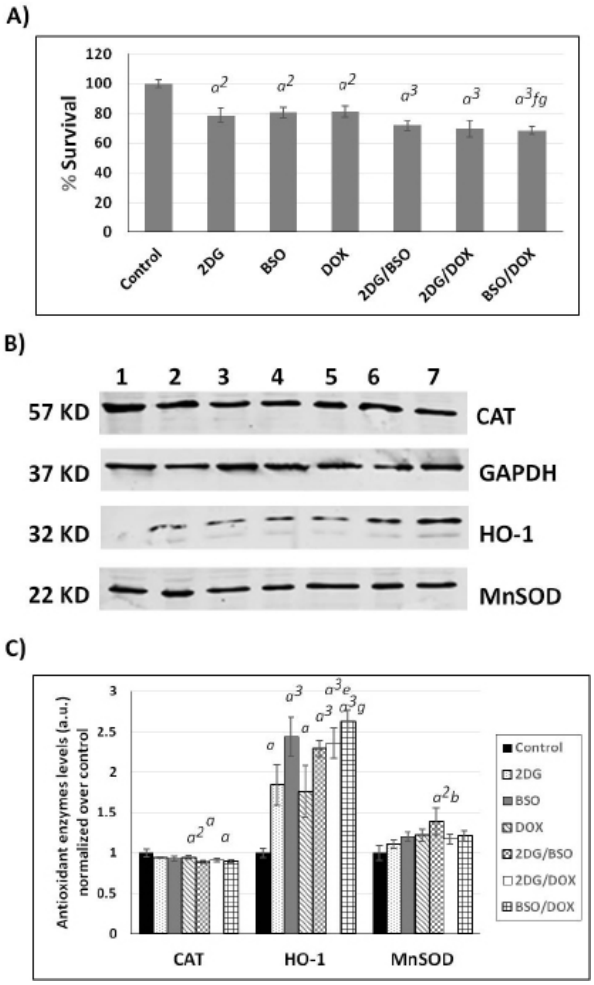

Figure 2. Oxidative Stress-causing Drugs Lead to Sub-Lethal Cytotoxicity and Changes in Antioxidant enzyme expression. **(A)** Effects of drugs on T47D breast cancer cell cytotoxicity. **(B)** Representative Western blot of whole lysates of control and treated T47D cells, blotted for CAT, HO-1, and MnSOD antioxidant enzymes. The experiment was repeated three times and the corresponding quantification is shown in **(C)**. Lane 1: control; lane 2: 2DG; lane 3: BSO; lane 4: DOX; lane 5: 2DG/BSO; lane 6: 2DG/DOX; lane 7: BSO/DOX. (C) Quantification of CAT, HO-1, and MnSOD levels (normalized to GAPDH) in control and treated cells. a $p<0.05$; a^2 $p<0.01$; a^3 $p<0.001$ versus control, b $p<0.05$ 2DG/BSO versus 2DG alone, e $p<0.05$ 2DG/DOX versus DOX alone, f $p<0.05$ BSO/DOX versus BSO alone, g $p<0.05$ BSO/DOX versus DOX alone

and 2DG/DOX and BSO/DOX drug combinations induced this expression as compared to DOX alone (Figure 2C). On the other hand, only 2DG/BSO drug combination induced the expression of MnSOD significanlty. The expression of catalase was reduced in all drug combinations as compared to control but not to individual drug treatment (Figure 2C).

Drug-treated T47D cells are characterized by a smaller cell area

To investigate the effect of drug treatment on the morphology of T47D cells, we measured cell length, width, length to width ratio (L/W ratio) and area of control and treated cells (Table 1). Cell width of treated cells decreased significantly when compared to control cells (Table 1). This in turn caused a decrease in cell area in

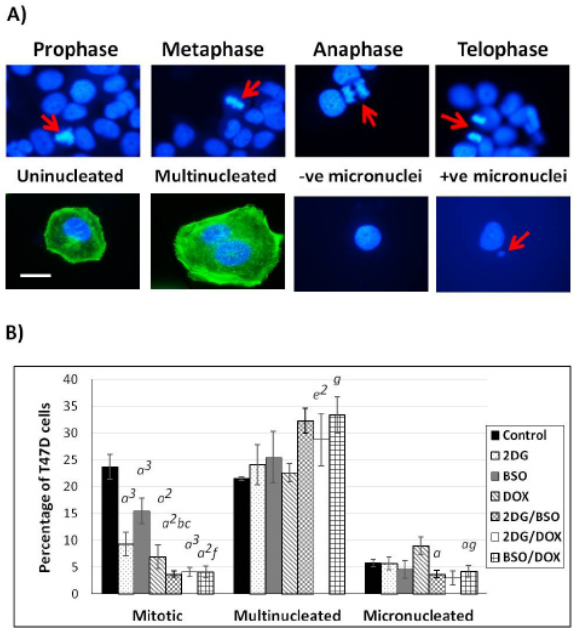

Figure 3. Disruption of Thiol Metabolism in T47D Cells Decreases Mitotic Index and Micronuclei Formation, and Increases Multinucleation. A) Microscope findings. B) Data are expressed as mean±SEM, n≥600 cells in each experiment, three independent experiments. a $p<0.05$; a^2 $p<0.01$; a^3 $p<0.001$ versus control, b $p<0.05$ 2DG/BSO versus 2DG alone, c $p<0.05$ 2DG/BSO versus BSO alone, e^2 $p<0.01$ 2DG/DOX versus DOX alone, f $p<0.05$ BSO/DOX versus BSO alone, g $p<0.05$ BSO/DOX versus DOX alone. Scale bar: 10 μm

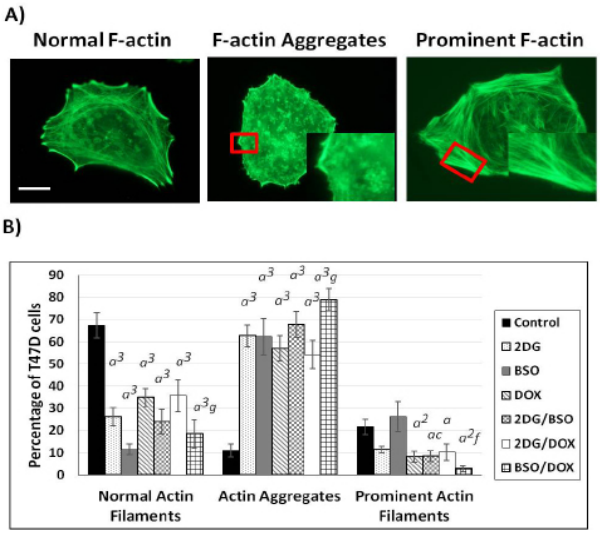

Figure 4. Treating T47D Breast Cancer Cells with 2DG, BSO, and DOX Individually or in Combination Causes Changes in F-actin structure. **(A)** Cells were categorized into three categories depending on their F-actin organization: normal F-actin, F-actin aggregates (magnified inset), and prominent F-actin (magnified inset) as stained with fluorescent-phalloidin. **(B)** Cells were scored as in (A) and presented as percentage of total cells. n≥100 cells in each experiment, three independent experiments. a $p<0.05$; a^2 $p<0.01$; a^3 $p<0.001$ versus control, c $p<0.05$ 2DG/BSO versus BSO alone, f $p<0.05$ BSO/DOX versus BSO alone, g $p<0.05$ BSO/DOX versus DOX alone. Scale bar: 10 μm

drug-treated cells when compared to control cells (Table 1), while the length and L/W ratio were not affected (Table1).

Table 1. Inducing Metabolic Oxidative Stress Reduces T47D Cell Width and Area

	Length (μm)	Width (μm)	Length/Width	Area (μm^2)
Control	95.8±7.2	70.2±9.3	1.5±0.1	7651.3±1883.3
2DG	80.0±5.5	60.8±3.3a	1.6±0.1	5934.2±881.1a
BSO	80.3±3.8	66.1±2.7a	1.3±0.04	5767.6±554.3a
DOX	77.9±2.6	58.3±3.8a	1.5±0.05	4847.5±509.9a
2DG/BSO	89.9±4.9	62.6±1.5a	1.4±0.06	6727.8±579.3a
2DG/DOX	88.7±4.1	56.1±1.6a	1.6±0.04	5326.6±281.7a
BSO/DOX	84.7±4.1	58.0±3.0af	1.5±0.06	5189.5±387.3a

Data are expressed as mean±SEM, n≥100 cells in each experiment, three independent experiments. a p<0.05 versus control, f p<0.05 BSO/DOX versus BSO alone

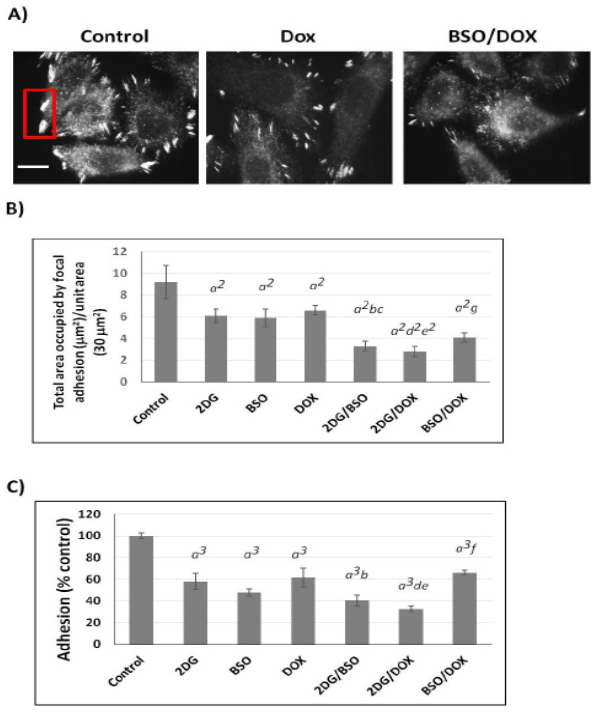

Figure 5. Oxidative Stress-causing Drugs Reduce T47D Cell Adhesion. (A) T47D breast cancer cells were stained for focal adhesion with mouse anti-paxillin primary antibody. The size and number of focal adhesions per unit area (30 μm^2; red box) were measured in NIS-Elements AR 4.10.00, six unit areas per cell. **(B)** Quantification of total area occupied by focal adhesion (μm^2)/30 μm^2 as: average number of focal adhesions/μm^2 X average size of focal adhesions. n≥25 cells in each experiment, three independent experiments. **(C)** Cells were subjected to collagen I adhesion assay. Average values of cells adherent to plastic (not shown) were subtracted from average values adherent to collagen I. Average values of control cells were reported to 100%. Four independent experiments each performed in triplicate. a^2 p<0.01; a^3 p<0.001 versus control, b p<0.05 2DG/BSO versus 2DG alone, c p<0.05 2DG/BSO versus BSO alone, d p<0.05; d^2 p<0.01 2DG/DOX versus 2DG alone, e p<0.05; e^2 p<0.01 2DG/DOX versus DOX alone, f p<0.05 BSO/DOX versus BSO alone, g p<0.05 BSO/DOX versus DOX alone. Scale bar: 10 μm

Drug combination affects mitotic parameters

Since mitosis and cytokinesis are actin-dependent processes, we wanted to investigate the effects of the drugs on certain mitotic parameters such as mitotic index (no. of mitotic cells/total no. of cells × 100%) (Figure 3A, B), percentage of multinucleation (no. of cells having two or more nuclei/total no. of cells × 100%) (Figure 3A, B), and percentage of micronucleation (no. of cells having fragments or whole chromosomes lagging behind in anaphase/total no. of cells × 100%) (Figure 3A, B). Drug treatment caused a significant reduction in the percentage of mitotic cells as compared to control cells (Figure 3B). Except for 2DG/DOX drug combination, the other two combinations (2DG/BSO and BSO/DOX) caused a significant decrease in the percentage of mitotic cells as compared to individual drug treatment.

Drug-treated cells exhibit changes in actin cytoskeleton

To determine if T47D-treated cells show changes in F-actin organization, T47D cells were treated with the different drugs for 24h, fixed and stained with fluorescent-phalloidin. Cells were observed and divided into three categories according to the structure of their actin cytoskeleton (Figure 4A) as described previously (Zebda et al., 2000; Sidani et al., 2007; Meng and Yue, 2014). Our results show that all of the drugs, used individually or in combination, significantly caused enhanced F-actin aggregates formation as compared to control cells accompanied by a significant decrease in normal and prominent F-actin (Figure 4B). Cells treated with the drug combination BSO/DOX showed the most enhanced actin aggregates formation (Figure 4B).

Disruption of thiol metabolism reduces T47D cell adhesion to collagen I

Changes in cell morphology and actin cytoskeleton structure suggested that drug treatment might have affected cell adhesion. We next investigated the effect of disrupting thiol metabolism on T47D cell adhesion (Figure 5). Control and drug-treated cells were stained with anti-paxillin antibody (Figure 5A) and the size and number of focal adhesions at cell periphery were measured per unit area (30 μm^2) (Figure 5A, B). Our results indicate that individual drug treatment decreased the total area occupied by focal adhesion as compared to control cells (Figure 5B). When drugs were used in combinations, the redcution in the total area occupied by focal adhesions decreased even more when compared to individual drug treatment (Figure 5B). In addition, control and treated cells were seeded onto collagen I-coated dishes, and adherent cells were quantified after 1 h (adhesion assay; (Estornes et al., 2007). We found that the percentage of adherent cells was less in drug-tretaed cells compared to control cells (Figure 5C). All drug combinations enhanced this effect on cell adhesion when compared to individual drug treatment.

Disruption of thiol metabolism reduces T47D breast cancer cells degrative ability

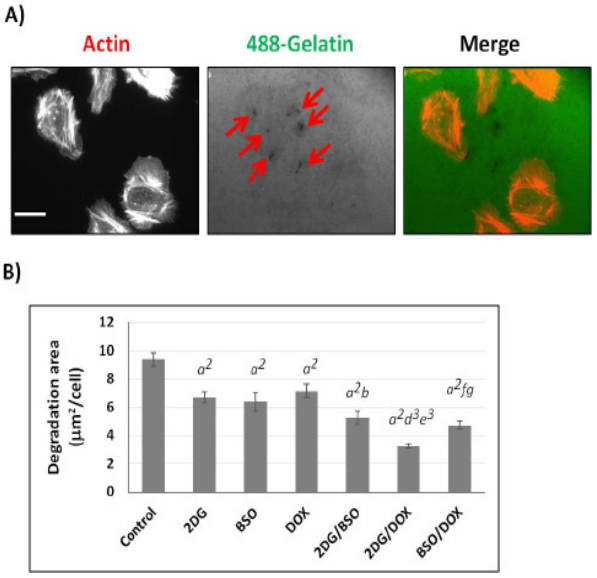

Figure 6. Disruption of Thiol Metabolism Affects Invadopodia Formation. **(A)** Cells were cultured on fluorescent gelatin-coated coverslips and stained with fluorescent-phalloidin to visualize invadopodia (arrows). **(B)** The degradation area of gelatin (μm^2) was quantified in NIS-Elements AR 4.10.00 and divided by number of cells in the same field and expressed as degradation area (μm^2)/cell. n≥25 cells in each experiment, three independent experiments. a^2 p<0.01 versus control, b p<0.05 2DG/BSO versus 2DG alone, d^3 p<0.001 2DG/DOX versus 2DG alone, e^3 p<0.001 2DG/DOX versus DOX alone, f p<0.05 BSO/DOX versus BSO alone, g p<0.05 BSO/DOX versus DOX alone. Scale bar: 10 μm

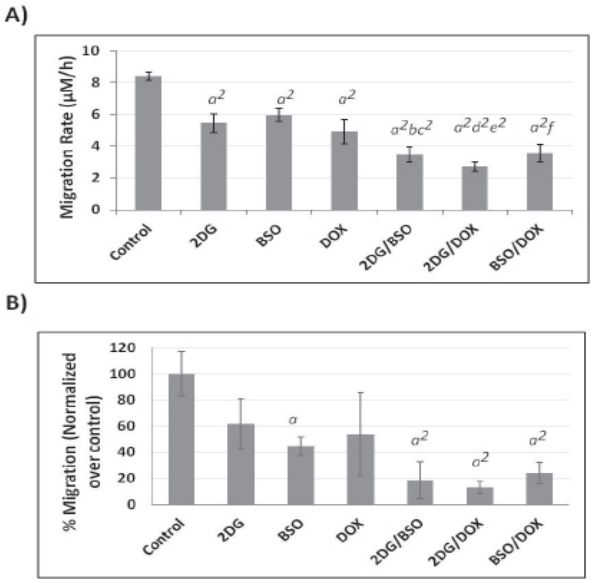

Figure 7. Inducing Metabolic Oxidative Stress in T47D Cells Reduces Cell Migration. **(A)** T47D breast cancer cells were grown into monolayers and wounds were made with a sterile tip. The wound area was measured at 0 hr and later at 6 h, and migration rate was expressed as μm/h. Three independent experiments each performed in triplicate. **(B)** Cells were serum-starved, seeded on collagen I-precoated filters and then subjected to migration assay. Cell migration is expressed as percent of control cells. Four independent experiments each performed in triplicate. a p<0.05; a^2 p<0.01 versus control, b p<0.05 2DG/BSO versus 2DG alone, c^2 p<0.01 2DG/BSO versus BSO alone, d^2 p<0.01 2DG/DOX versus 2DG alone, e^2 p<0.01 2DG/DOX versus DOX alone, f p<0.05 BSO/DOX versus BSO alone

To examine the effects of drug treatment on T47D cells ability to degrade the extracellular matrix (ECM), cells were grown on fluorescent gelatin and the proteolytic activity (dark non-fluorescent areas; Figure 6A) was measured (Figure 6B). Drug treatment reduced the degradative ability of cells as compared to control and all drug combinations reduced this ability when compared to individual drug treatments (Figure 6B).

Metabolic oxidative stress decreases the rate of migration of T47D breast cancer cells

Since disruption of thiol metabolism affected actin organization and cell adhesion, we next analyzed the effect of drug treatment on the migration of T47D breast cancer cells. The wound healing assay measures cell directed migration as a response to clearing of cells in a monolayer (Montanez et al., 2007). The migration rate of cells treated individually decreased significantly when compared to the control (p<0.01) (Figure 7A). Treating T47D breast cancer cells with the combination therapy enhanced this reduction (Figure 7B). In addition, we measured the number of control and treated cells migrating across type I collagen-coated 8 μm filters (migration assay). Treating T47D cells with BSO or the combination therapy reduced T47D cell migration by almost 80% compared to control cells (Figure 7B).

Discussion

Breast cancer has become the second leading malignancy among women in both developing and developed countries (Li et al., 2013). Cancer cell metastasis is the most sever stage in cancer and is the main cause of morbidity in cancer patients (Gupta and Massague, 2006). A major challenge in cancer therapy is to discover means to inhibit tumor cell migration from primary site to other body organs (i.e. inhibit metastasis) (Hayot et al., 2006; Hegde et al., 2013).

As in most other solid tumors, breast cancer metastatic phase rather than the primary lesion is responsible for the vast majority of patients' morbidity and mortality (Dong et al., 2009). Therefore, metastasis continues to be the main obstacle to the effective treatment of breast cancer, and there is an urgent need to develop novel therapeutics to inhibit this process.

Recently, it has been noted that metastatic cells have an increased dependency on glycolytic pathways while down-regulating pathways involved in oxidative phosphorylation (Sottnik et al., 2011; Jin and Wei, 2014). This is a further enhancement of the Warburg effect which states that tumor cells become dependent on glycolysis and decrease their oxygen utilization as they become more aggressive (Zhao et al., 2013; Jin and Wei, 2014).

These metabolic differences arise as a result of a fundamental defect in the tumor mitochondrial electron transport chain which leads to increased steady state levels of pro-oxidants (Nakashima et al., 1984). Previous studies suggest that breast cancer patients are exposed to conditions of oxidative stress (Noda and Wakasugi, 2001). As a compensatory mechanism in response to this increase in ROS, cancer cells exhibit an increase in glucose

metabolism by forming pyruvate and NADPH which are believed to function in hydroperoxide detoxification (Nakashima et al., 1984). Accordingly, the increased dependency of metastatic cancer cells on glucose metabolism is an attractive target for treatment strategies since these pathways are common to tumor cells.

Several studies have shown that glucose deprivation can induce cytotoxicity in transformed human cell types via metabolic oxidative stress (Lee et al., 1998; Lin et al., 2003). In our previous study, we demonstrated that the inhibition of glycolysis using 2DG induced cytotoxicity in T47D breast cancer cells (Ahmad et al., 2010). This is consistent with previous studies in which it was shown that 2DG induced growth inhibition and cytotoxicity in MDA-MB231 breast cancer cells (Andringa et al., 2006), and FaDu squamous cell carcinoma (Simons et al., 2007).

On the other hand, when combining 2DG with DOX a significant cell killing in rapidly dividing T47D cells compared with 2DG or DOX alone was observed (Ahmad et al., 2010). This is also consistent with previous studies, suggesting that 2DG may potentially increase the efficacy of standard chemotherapeutic drugs (Maschek et al., 2004). Furthermore, we previously reported that BSO, a potent inhibitor of glutathione biosynthesis, sensitized T47D cells to apoptosis induced by 2DG and DOX, which suggests that inhibition of GSH synthesis further enhanced the oxidative stress induced by these drugs (Ahmad et al., 2010).

The role of ROS in controlling vital cellular processes has emerged in the last decade (Moldovan et al., 2006). These molecules function as signaling molecules in many physiological processes including cell growth, gene expression, and cell migration (Moldovan et al., 2006; Shinohara et al., 2007). The role of ROS in cell migration depends on the type of the ROS, dose, production site and cell type (Luanpitpong et al., 2010).

In the current study we validated our previous findings in terms of being able to induce metabolic oxidative stress, and our results were consistent with what has been published previously (Ahmad et al., 2010) (Figure 1 and 2). Accordingly, we hypothesized that 2DG or DOX can act synergistically with inhibitors of hydroperoxide detoxification (i.e. BSO) to produce oxidative stress and to revert highly metastatic cancer cells to a less aggressive phenotype, leading to inhibition of metastasis.

Metastasis is a multistep process characterized by cellular deformation involving the formation of protrusions and new adhesions to surfaces as well as cellular contractility, which is required for rear retraction and cellular transmigration (Menhofer et al., 2014). In all of these processes, actin cytoskeleton plays a pivotal role and undergoes a constant polymerization and depolymerization to form protrusions and stress fibers (Sakthivel et al., 2012; Tahtamouni et al., 2013).

ROS have a key regulatory effect on actin cytoskeleton, which has a dynamic structure that participates in cell motility. It has been reported that oxidation of β\γ (non-muscle forms of actin) leads to complete loss of polymerization (Lassing et al., 2007). Another study reported that the increase in the ROS superoxide (O_2-) causes carbonylation of actin, leading to loss of lamellopdia formation (Barth et al., 2009). In addition, ROS regulate actin reorganization via Rac1-mediated ROS production from NADPH oxidase, which is responsible for electron transfer to molecular oxygen leading to superoxide production (Alexandrova et al., 2006). The prevention of superoxide formation from NADPH oxidase reduces cell migration in hypoxic endothelial cell (EC) (Moldovan et al., 2006).

Therefore, we first examined alterations in actin cytoskeleton organization and cell shape changes. In T47D cells, actin cytoskeleton exists in three different categories: normal F-actin, F-actin aggregates, and prominent F-actin (stress fibers) (Figure 4A). Our results show that all of the drugs used individually or in combination, significantly enhanced F-actin aggregates formation as compared to control cells accompanied by a significant decrease in normal and prominent F-actin (Figure 4B). The combination of BSO/DOX elicited the most enhanced actin aggregate formation (Figure 4B). F-actin aggregate formation might indicate enhanced myosin II activities (Wiggan et al., 2012).

Actin cytoskeleton is also involved in regulating the cell cycle, during which it undergoes drastic changes and remodeling (Heng and Koh, 2010). Thus, the regulation of actin cytoskeleton and the cell cycle progression appears to be connected (Heng and Koh, 2010). Our result show that disruption of actin cytoskeleton dynamics was accompined with a delay in entry to mitosis (Figure 3B).

ROS regulate cell migration via regulating many proteins such as integrins, small Rho GTPase family, focal adhesion-forming proteins, and extracellular matrix degrading enzymes such as metalloproteinase (MMP) (Luanpitpong et al., 2010). An important observation of our study is that individual or combination treatments induced morphological changes in T47D cells (Table 1). T47D cells, when grown on tissue culture dishes, display typical epithelioid characteristics; cells are flat and polygonal in shape and are very adhesive to the plastic substratum (Shiu and Paterson, 1984). We found that treated cells became smaller and round compared to control cells (Table 1). Consequently, cell adhesion and invasion were also dramatically impaired (Figure 5, 6, and 7).

Our data show that the percentage of adherent cells was less in drug-treated cells compared to control cells (Figure 5C). All drug combinations enhanced this effect on cell adhesion when compared to individual drug treatment (Figure 5C). Focal adhesions are sites of large macromoleuclar assemblies containing integrins with linkages to cytoplasmic actin bundles and collagen (Chen et al., 2003; Zaidel-Bar et al., 2004). Since our drug treatment increased F-actin aggregate formation with a reduction in stress fiber formation, this in turn reduced focal adhesion formation (Figure 5A). Focal adhesions provide a tension force needed for the forward movement of cell body.

In addition, drug treatment reduced the degradative ability of cells to ECM as compared to control, and all drug combinations reduced this ability when compared to individual drug treatments (Figure 6). Different reports have shown that successful tumor cell metastasis requires

cells to adhere to blood vessels of host organ (Korb et al., 2004). Thus, impairing tumor cell ability to form stable adhesion to vessel wall would help in preventing tumor ability to migrate, invade, and metastasize. Our data presented in Figure 5 indicate that drug treatment decreased T47D cell adhesion, leading to decreased migration rate (Figure 7) (Tahtamouni et al., 2013).

The results presented here indicate that the anti-metastatic properties of the different drugs used in the current study, may be mediated by impaired actin polymerization and cytoskeletal control. Our findings may contribute to the understanding of the relationship between metabolic oxidative stress and breast cancer cell metastasis progression. In addition, our findings provide a strong support for the potential therapeutic use of sub-lethal metabolic oxidative stress mediated by glucose and glutathione depletion.

Acknowledgements

The authors are grateful for the Deanship of Research and Graduate Studies, the Hashemite University. This work was supported in part by L'OREAL-UNESCO For Women in Science Pan-Arab Regional Fellowship (LHT), and a grant from King Hussein Institute for Biotechnology and Cancer (LHT).

References

American Cancer Society. (2014). Breast cancer: detailed guide.

Ahmad I, Mustafa E, Mustafa N, et al (2010). 2DG enhances the susceptibility of breast cancer cells to doxorubicin. *Cen Eur J Biol*, **5**, 739-48.

Ahmad I, Aykin-Burns N, Sim J, et al (2005). Mitochondrial and H_2O_2 mediate glucose deprivation-induced stress in human cancer cells. *J Biol Chem*, **280**, 4254-63.

Alexandrova A, Kopnin P, Vasiliev J, et al (2006). ROS up-regulation mediates Ras-induced changes of cell morphology and motility. *Exp Cell Res*, **312**, 2066-73.

Anderson E (1985). Determination of glutathione and glutathione disulfide in biological samples. *Methods Enzymol*, **113**, 548-55.

Andringa K, Coleman M, Aykin-Burns N, et al (2006). Inhibition of glutamate cysteine ligase activity sensitizes human breast cancer cells to the toxicity of 2-deoxy-D-glucose. *Cancer Res*, **66**, 1605-10.

Artym V, Yamada K, Mueller S (2009). ECM degradation assays for analyzing local cell invasion. *Methods Mol Biol*, **522**, 211-9.

Averill-Bates D, Przybytkowski E (1994). The role of glucose in cellular defences against cytotoxicity of hydrogen peroxide in Chinese hamster ovary cells. *Arch Biochem Biophys*, **312**, 52-8.

Barth B, Stewart-Smeets S, Kuhn T (2009). Proinflammatory cytokines provoke oxidative damage to actin in neuronal cells mediated by Rac1 and NADPH oxidase. *Mol Cell Neurosci*, **41**, 274-85.

Bertazzoli C, Bellini O, Magrini U et al (1979). Quantitative experimental evaluation of adriamycin cardiotoxicity in the mouse. *Cancer Treat Reports*, **63**, 1877-83.

Chen Q, Vazquez E, Moghaddas S, et al (2003). Production of reactive oxygen species by mitochondria: central role of complex III. *J Biol Chem*, **278**, 36027-31.

Coleman M, Asbury C, Daniels D, et al (2008). 2-deoxy-D-glucose causes cytotoxicity, oxidative stress, and radiosensitization in pancreatic cancer. *Free Radic Biol Med*, **44**, 322-31.

Dong F, Budhu A, Wang X (2009). Translating the metastasis paradigm from scientific theory to clinical oncology. *Clin Cancer Res*, **15**, 2588-93.

Estornes Y, Gay F, Gevrey J, et al (2007). Differential involvement of destrin and cofilin-1 in the control of invasive properties of Isreco1 human colon cancer cells. *Int J Cancer*, **121**, 2162-71.

Gavino V, Miller J, Ikharebha S, et al (1981). Effect of polyunsaturated fatty acids and antioxidants on lipid peroxidation in tissue cultures. *J Lipid Res*, **22**, 763-9.

Gille L, Nohl H (1997). Analyses of the molecular mechanism of adriamycin-induced cardiotoxicity. *Free Radic Biol Med*, **23**, 775-82.

Griffith O (1980). Determination of glutathione and glutathione disulfide using glutathione reductase and 2-vinylpyridine. *Anal Biochem*, **106**, 207-12.

Gupta G, Massague J (2006). Cancer metastasis: building a framework. *Cell*, **127**, 679-95.

Gurudath S, Ganapathy K, Pai A, et al (2012). Estimation of superoxide dismutase and glutathione peroxidase in oral submucous fibrosis, oral leukoplakia and oral cancer--a comparative study. *Asian Pac J Cancer Prev*, **13**, 4409-12.

Hayot C, Debeir O, Van Ham P, et al (2006). Characterization of the activities of actin-affecting drugs on tumor cell migration. *Toxicol Appl Pharmacol*, **211**, 30-40.

Hegde M, Mali A, Chandorkar S (2013). What is a cancer cell? Why does it metastasize? *Asian Pac J Cancer Prev*, **14**, 3987-9.

Heng Y, Koh C (2010). Actin cytoskeleton dynamics and the cell division cycle. *Int J Biochem Cell Biol*, **42**, 1622-33.

Jin L, Wei C (2014). Role of microRNAs in the Warburg effect and mitochondrial metabolism in cancer. *Asian Pac J Cancer Prev*, **15**, 7015-9.

Korb T, Schluter K, Enns A, et al (2004). Integrity of actin fibers and microtubules influences metastatic tumor cell adhesion. *Exp Cell Res*, **299**, 236-247.

Lassing I, Schmitzberger F, Bjornstedt M, et al (2007). Molecular and structural basis for redox regulation of beta-actin. *J Mol Biol*, **370**, 331-48.

Lee D, Kang S (2013). Reactive oxygen species and tumor metastasis. *Mol Cells*, **35**, 93-8.

Lee Y, Galoforo S, Berns C , et al (1998). Glucose deprivation-induced cytotoxicity and alterations in mitogen-activated protein kinase activation are mediated by oxidative stress in multidrug-resistant human breast carcinoma cells. *J Biol Chem*, **273**, 5294-9.

Li X, Kong X, Wang Y, et al (2013). BRCC2 inhibits breast cancer cell growth and metastasis *in vitro* and *in vivo* via downregulating AKT pathway. *Cell Death Dis*, **4**, 757.

Lin X, Zhang F, Bradbury C, et al (2003). 2-deoxy-D-glucose-induced cytotoxicity and radiosensitization in tumor cells is mediated via disruptions in thiol metabolism. *Cancer Res*, **63**, 3413-7.

Luanpitpong S, Talbott S, Rojanasakul Y, et al (2010). Regulation of lung cancer cell migration and invasion by reactive oxygen species and caveolin-1. *J Biol Chem*, **285**, 38832-40.

Lykkesfeldt J (2007). Malondialdehyde as biomarker of oxidative damage to lipids caused by smoking. *Clinica Chimica Acta*, **380**, 50-8.

Green M, Graham M, O'Donovan R, et al (2006). Subcellular compartmentalization of glutathione: Correlations with parameters of oxidative stress related to genotoxicity. *Mutagenesis*, **21**, 383-90.

Maschek G, Savaraj N, Priebe W, et al (2004). 2-deoxy-D-

glucose increases the efficacy of adriamycin and paclitaxel in human osteosarcoma and non-small cell lung cancers *in vivo*. *Cancer Res*, **64**, 31-4.

Meng X, Yue S (2014). Dexamethasone disrupts cytoskeleton organization and migration of T47D human breast cancer cells by modulating the AKT/mTOR/RhoA pathway. *Asian Pac J Cancer Prev*, **15**, 10245-50.

Menhofer M, Kubisch R, Schreiner L, et al (2014). The actin targeting compound chondramide inhibits breast cancer metastasis via reduction of cellular contractility. *PLoS ONE*, **9**, 112542.

Meredith M, Reed D (1982). Status of the mitochondrial pool of glutathione in the isolated hepatocyte. *J Biol Chem*, **257**, 3747-53.

Moldovan L, Mythreye K, Goldschmidt-Clermont P, et al (2006). Reactive oxygen species in vascular endothelial cell motility. Roles of NAD(P)H oxidase and Rac1. *Cardiovasc Res*, **71**, 236-46.

Montanez E, Piwko-Czuchra A, Bauer M, et al (2007). Integrin. (2nd edition ed.). Academic Press, San Diego.

Mosmann T (1983). Rapid colorimetric assay for cellular growth and survival: Application to proliferation and cytotoxicity assays. *J Immunol Methods*, **65**, 55-63.

Mu X, Shi W, Sun L, et al (2012). Pristimerin inhibits breast cancer cell migration by up- regulating regulator of G protein signaling 4 expression. *Asian Pac J Cancer Prev*, **13**, 1097-104.

Muyderman H, Nilsson M, Sims N (2004). Highly selective and prolonged depletion of mitochondrial glutathione in astrocytes markedly increases sensitivity to peroxynitrite. *J Neurosci*, **24**, 8019-28.

Nakashima R, Paggi M, Pedersen P (1984). Contributions of glycolysis and oxidative phosphorylation to adenosine 5´-triphosphate production in AS-30D hepatoma cells. *Cancer Res*, **44**, 5702-6.

Noda N, Wakasugi H (2001). Cancer and oxidative stress (Vol. 44).

Nourazarian A, Kangari P, Salmaninejad A (2014). Roles of oxidative stress in the development and progression of breast cancer. *Asian Pac J Cancer Prev*, **15**, 4745-51.

Oberley L, Buettner G (1979). Role of superoxide dismutase in cancer: a review. *Cancer Res*, **39**, 1141-9.

Ohkawa H, Ohishi N, Yagi K (1979). Assay for lipid peroxides in animal tissues by thiobarbituric acid reaction. *Anal Biochem*, **95**, 351-8.

Ortega A, Mena S, Estrela J (2010). Oxidative and nitrosative stress in the metastatic microenvironment. *Cancers (Basel)*, **2**, 274-304.

Pani, Galeotti T, Chiarugi P (2010). Metastasis: cancer cell's escape from oxidative stress. *Cancer Metastasis Rev*, **29**, 351-78.

Sakthivel K, Prabhu V, Guruvayoorappan C (2012). WAVEs: a novel and promising weapon in the cancer therapy tool box. *Asian Pac J Cancer Prev*, **13**, 1719-22.

Schumacker P (2006). Reactive oxygen species in cancer cells: live by the sword, die by the sword. *Cancer Cell*, **10**, 175-6.

Shinohara M, Shang W, Kubodera M, et al (2007). Nox1 redox signaling mediates oncogenic Ras-induced disruption of stress fibers and focal adhesions by down-regulating Rho. *J Biol Chem*, **282**, 17640-8.

Shiu R, Paterson J (1984). Alteration of cell shape, adhesion, and lipid accumulation in human breast cancer cells (T-47D) by human prolactin and growth hormone. *Cancer Res*, **44**, 1178-86.

Sidani M, Wessels D, Mouneimne G, et al (2007). Cofilin determines the migration behavior and turning frequency of metastatic cancer cells. *J Cell Biol*, **179**, 777-91.

Sies H (1997). Oxidative stress: oxidants and antioxidants. *Exp Physiol*, **82**, 291-5.

Simons A, Ahmad I, Mattson D, et al (2007). 2-Deoxy-D-glucose combined with cisplatin enhances cytotoxicity via metabolic oxidative stress in human head and neck cancer cells. *Cancer Res*, **67**, 3364-70.

Siveski-Iliskovic N, Hill M, Chow D, et al (1995). Probucol protects against adriamycin cardiomyopathy without interfering with its antitumor effect. American heart association. *Circulation*, **91**, 10-5.

Sottnik J, Lori J, Rose B, et al (2011). Glycolysis inhibition by 2-deoxy-D-glucose reverts the metastatic phenotype *in vitro* and *in vivo*. *Clin Exp Metastasis*, **28**, 865-75.

Tahtamouni L, Shaw A, Hasan M, et al (2013). Non-overlapping activities of ADF and cofilin-1 during the migration of metastatic breast tumor cells. *BMC Cell Biol*, **14**, 45-61.

Takanashi S, Bachur N (1976). Adriamycin metabolism in man evidence from urinary metabolites. *Drug Metabol Dispos*, **4**, 79-87.

Toyokuni S, Okamoto K, Yodoi J, et al (1995). Persistent oxidative stress in cancer. *FEBS Lett*, **358**, 1-3.

Wiggan O, Shaw A, DeLuca J, et al (2012). ADF/cofilin regulates actomyosin assembly through competitive inhibition of myosin II binding to F-actin. *Develop Cell*, **22**, 530-43.

Wold L, II N, Ren J (2005). Doxorubicin induces cardiomyocyte dysfunction via a p38 MAP kinase-dependent oxidative stress mechanism. *Cancer Detect Prev*, **29**, 294-9.

Wu D, Cederbaum A (2003). Alcohol, oxidative stress, and free radical damage. *Alcohol Res Health*, **27**, 277-84.

Zaidel-Bar R, Cohen M, Addadi L, Geiger B (2004). Hierarchical assembly of cell-matrix adhesion complexes. *Biochem Soc Trans*, **32**, 416-20.

Zebda N, Bernard O, Bailly M, et al (2000). Phosphorylation of ADF/cofilin abolishes EGF-induced actin nucleation at the leading edge and subsequent lamellipod extension. *J Cell Biol*, **151**, 1119-28.

Zhang J, Rubio V, Zheng S, et al (2009). Knockdown of OLA1, a regulator of oxidative stress response, inhibits motility and invasion of breast cancer cells. *J Zhejiang Univ Sci B*, **10**, 796-804.

Zhao Y, Butler E, Tan M (2013). Targeting cellular metabolism to improve cancer therapeutics. *Cell Death Dis*, **4**, 532.

Zhou S, Starkov A, Froberg M, et al (2001). Cumulative and irreversible cardiac mitochondrial dysfunction induced by doxorubicin. *Cancer Res*, **61**, 771-7.